Available online at www.sciencedirect.com

SciVerse ScienceDirect

Ceramics International 38 (2012) 3367–3375

CERAMICS INTERNATIONAL

www.elsevier.com/locate/ceramint

Effect of hafnium on the microstructure, dielectric and ferroelectric properties of $Ba[Zr_{0.2}Ti_{0.8}]O_3$ ceramics

Wei Cai [a,b,*], Chunlin Fu [a,c], Jiacheng Gao [b], Zebin Lin [a], Xiaoling Deng [a]

[a] School of Metallurgical and Materials Engineering, Chongqing University of Science and Technology, Chongqing 401331, China
[b] College of Materials Science and Engineering, Chongqing University, Chongqing 400044, China
[c] State Key Laboratory of Electronic Thin Films and Integrated Devices, University of Electronic Science and Technology of China, Chengdu 610054, China

Received 3 August 2011; received in revised form 15 December 2011; accepted 19 December 2011
Available online 28 December 2011

Abstract

Hafnium (Hf)-doped $Ba[Zr_{0.2}Ti_{0.8}]O_3$ (BZT) ceramics were prepared by the conventional solid-state reaction method. The microstructure, dielectric and ferroelectric properties of Hf-doped BZT ceramics have been investigated. Hf^{4+} ions enter the perovskite-type cubic structure to substitute for Ti^{4+} ions on the B sites and lead to the increase of the lattice parameter. Addition of hafnium can restrain grain growth in the BZT ceramics. Hf-doped BZT ceramics have ferroelectric properties with diffuse phase transition. Hf^{4+} ions can reduce dielectric loss of BZT ceramics. As Hf content increases, the remnant polarization begins to increase to the maximum and then decrease, while the coercive field begins to decrease to the minimum and then increase. The remnant polarization, saturation polarization and coercive field decrease with the rise of measurement temperature.

Keywords: B. Microstructure; C. Dielectric; Ferroelectric; D. Barium zirconate titanate; Hafnium; Ceramic

1. Introduction

Barium titanate ($BaTiO_3$) is the most common ferroelectric oxide with the perovskite ABO_3 structure, which is used as a capacitor because of its high dielectric constant [1,2]. In order to reduce the dielectric loss at low frequency, ZrO_2 was doped into barium titanate to substitute for Ti^{4+} ions on the B sites and form $Ba[Zr_xTi_{1-x}]O_3$ (BZT) [3–5]. BZT has attracted great attention for its potential applications for the microwave technology, due to its high dielectric constant, low dielectric loss and large tunability [6,7].

In recent years, most studies are focused on the preparation, microstructure and dielectric properties of BZT ceramics and thin films [8–11]. Microstructure, dielectric, piezoelectric and ferroelectric properties of BZT materials can be modified by a wide variety of substitutions possible at Ba^{2+} on the A sites or Ti^{4+} or Zr^{4+} on the B sites independently or simultaneously in perovskite structure [12–26]. These dopants can be isovalent or heterovalent. The heterovalent substitutions cause charge imbalance and create vacancies on the A site or B site or oxygen sublattice or generate holes to maintain electrical charge neutrality. Diez-Betriu et al. [12] reported that a dramatic fall in the transition temperature occurs when BZT ceramics are doped with A-site deficient rare-earth (La, Pr, Nd, Gd). Moreover, diffusivity degree of the phase transition increases and a relaxor-type behavior is induced due to both the increment of the lanthanide content and the increase of the ionic radius of the dopant element. Mahajan et al. [20] found that the degree of relaxation behavior and the remnant polarization of Bi-doped $Ba[Zr_{0.05}Ti_{0.95}]O_3$ ceramics increase with bismuth concentration. The rare-earth ions (La, Ce and Dy) can enter the perovskite structure to substitute for A-site Ba^{2+} ions and inhibit the grain growth of BZT [22]. The dielectric constant, dielectric loss, tunability and leakage current density of BZT thin films decrease with the increase of rare-earth ions concentration. The Curie temperature of $[Ba_{1-3x/2}Bi_x][Zr_yTi_{1-y}]O_3$ ceramics decreases with increasing x and the ferroelectric behavior of samples with $0.075 \leq x \leq 0.1$ is a relaxor-like behavior [25]. Furthermore, Li et al. [26] prepared $[Ba_{1-x}Ca_x][Ti_{0.95}Zr_{0.05}]O_3$ ceramics by

* Corresponding author. Permanent address: School of Metallurgical and Materials Engineering, Chongqing University of Science and Technology, Huxi Town, Shapingba, Chongqing 401331, China. Tel.: +86 23 65023479; fax: +86 23 65023706.
E-mail address: caiwei_cqu@163.com (W. Cai).

0272-8842/$36.00
doi:10.1016/j.ceramint.2011.12.047

solid-state reaction and found that the temperature of orthorhombic-tetragonal phase transition shifts toward room temperature with the increase of Ca content and enhanced ferroelectric properties are obtained for the sample of $x = 0.08$. It is implied that proper doping can improve the dielectric properties of BZT materials. Although effects of doping hafnium on the $BaTiO_3$ materials were investigated [27–30], the leakage current decreases by almost four orders of magnitude with a hafnium substitution of 40% [27]. The chemical property of hafnium is very much similar to that of zirconium, but its atomic weight of Hf (178.5 g/mol) is much larger than that of Zr (91.2 g/mol). As a result, the partial substitution of Ti or Zr on B sites in BZT by Hf might provide an alternative to effectively improve the properties of BZT. However, the effects of Hf-doped BZT ceramics have not yet been reported. In this paper, we prepared Hf-doped $Ba[Zr_{0.2}Ti_{0.8}]O_3$ ceramics by the conventional solid-state reaction method and investigated the effects of hafnium on microstructure, dielectric and ferroelectric properties.

2. Experimental details

$Ba[Zr_{0.2}Ti_{0.8}]O_3$ ceramics, pure and doped with 0.5–3.0 wt.% Hf, were prepared by the conventional solid-state reaction method. The starting raw chemicals were high purity barium carbonate [$BaCO_3$] (≥99.9%, Sinopharm Group Co. Ltd.), titanium oxide [TiO_2] (≥99.9%, Sinopharm Group Co. Ltd.), zirconium oxide [ZrO_2] (≥99.5%, Sinopharm Group Co. Ltd.) and hafnium oxide [HfO_2] (≥99.9%, Beijing Founde Star Science and Technology Co. Ltd.) powders. After weighing respectively in stoichiometric proportions, $BaCO_3$, TiO_2, ZrO_2 and HfO_2 were added into a ball milling jar, and then milled for 2 h in distilled water and zirconia media. After the slurry was dried, the mixture consisting of $BaCO_3$, TiO_2, ZrO_2 and HfO_2 was calcined in an alumina crucible at 1100 °C for 4 h in air and $BaCO_3$, TiO_2, ZrO_2 and HfO_2 reacted to form Hf-doped $Ba[Zr_{0.2}Ti_{0.8}]O_3$ powders. The calcined powders were remilled for 2 h and then dried. The powders added with 7 wt.% binders were compacted into disk-shaped pellets with a diameter of 10.0 mm and thickness of 1.0 mm at 20 MPa pressure. The green pellets of both pure and Hf-doped $Ba[Zr_{0.2}Ti_{0.8}]O_3$ were sintered at 1350 °C for 2 h in air.

The crystal structure of the ceramic samples was examined at room temperature by X-ray diffraction (XRD) (DX-2700 model, Dandong Fangyuan, China). Surface morphology of the sintered samples was examined by scanning electron microscope (SEM) (S-3700N model, Hitachi, Tokyo, Japan).

In order to measure the dielectric properties, silver paste was painted on the polished samples and fired at 830 °C for 15 min as the electrodes. The capacitances of the ceramics were determined by inductance (L), capacitance (C) and resistance (R) meter (LCR) (HP4980A model, Agilent, USA) at 1 V/mm from −60 °C to 150 °C with 0.5 °C/min. The dielectric constant was calculated using the following equation:

$$\varepsilon = \frac{Cd}{\varepsilon_0 A} \quad (1)$$

where C is the capacitance (F), ε_0 is the free space dielectric constant value (8.855×10^{-12} F/m), A represents the capacitor area (m^2) and d represents the thickness (m) of the ceramics. The polarization–electric field (P–E) hysteresis characteristics were performed out using a ferroelectric test system (TF2000e, aixACCT, Germany).

3. Results and discussion

3.1. Crystal structure

XRD patterns of pure and Hf-doped BZT ceramics are shown in Fig. 1. Firstly, the XRD patterns are virtually the same and show only single phase perovskite structure without the evidence of the second phase. It implies that Hf^{4+} ions have entered the unit cell maintaining the perovskite structure of solid solution. XRD patterns of pure and Hf-doped BZT ceramics are in agreement with the respective joint committee on powder diffraction standards (JCPDS file no. 36-0019) and the literatures [14,31]. Secondly, the diffraction peaks of samples move to the lower angle side with the increase of Hf content. The systematic shift of the XRD peaks indicates the solid solubility of Hf in BZT lattice and the increase in lattice parameter with the increasing of Hf content. The Hf content dependence of lattice parameters of pure and Hf-doped BZT ceramics is shown in Fig. 2. It can be explained that the Hf^{4+} ions substitute for Ti^{4+} ions on the B sites of the BZT lattice. The ionic radius of Hf^{4+} (0.079 nm) is larger than that of Ti^{4+} (0.068 nm).

3.2. Surface morphology

The SEM micrographs of pure and Hf-doped $Ba[Zr_{0.2}Ti_{0.8}]O_3$ ceramics are shown in Fig. 3. It is found that all the sintered ceramic samples are dense. The average grain sizes of Hf-doped BZT ceramics by lineal intercept procedure are ~85 μm, ~90 μm, ~4 μm, ~3 μm and ~2 μm as Hf content increases from 0 to 0.5 wt.%, 1.5 wt.%, 2.0 wt.% and 3.0 wt.%, respectively. This result

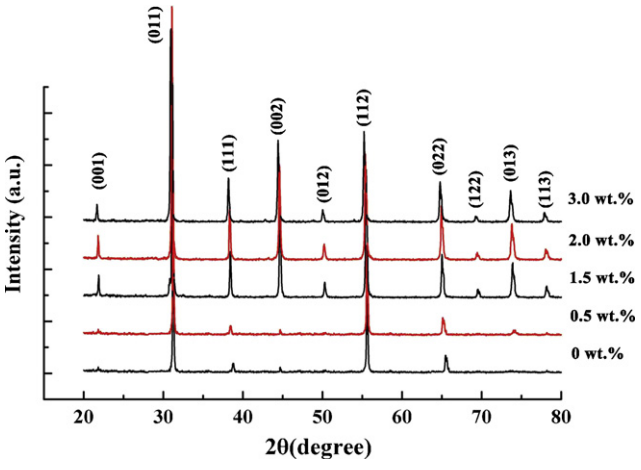

Fig. 1. XRD patterns of pure and Hf-doped BZT ceramics at room temperature.

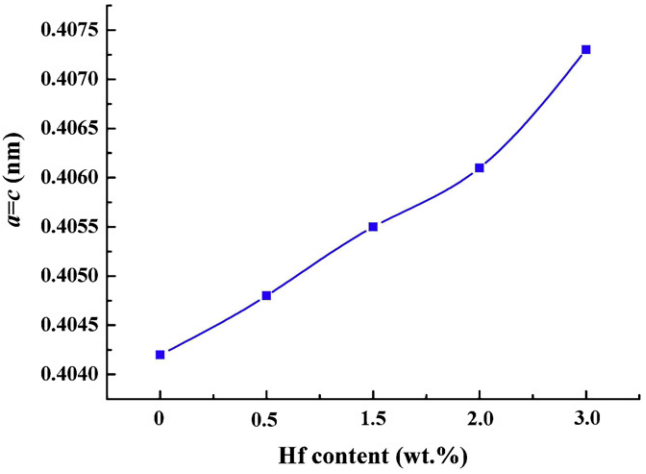

Fig. 2. Hf content dependence of lattice parameter for Hf-doped BZT ceramics.

suggests that the incorporation of Hf^{4+} ions can restrain grain growth in the BZT ceramics and the grain size decreases sharply when Hf content is above 0.5 wt.%. The growth mechanism occurs by the grain boundary motion due to a reduction of the total grain boundary surface energy. The thermal energy leads to an increase in the diffusion rate and consequently intensifies the formation of necks between grains [32]. The reason for the decrease of grain size can be explained based on the ionic radii of Ti^{4+} and Hf^{4+}. Since ionic radius and atomic weigh of Hf are larger than that of Ti, larger amounts of Hf^{4+} result in less mobility of the ions and grain size decreases [33]. The similar results are shown in Hf-doped $BaTiO_3$ [27,34]. Moreover, there is coexistence of small and large grains for pure BZT and BZT ceramics with 0.5 wt.% Hf, and the grain of the BZT ceramics becomes more uniform as hafnium content increases.

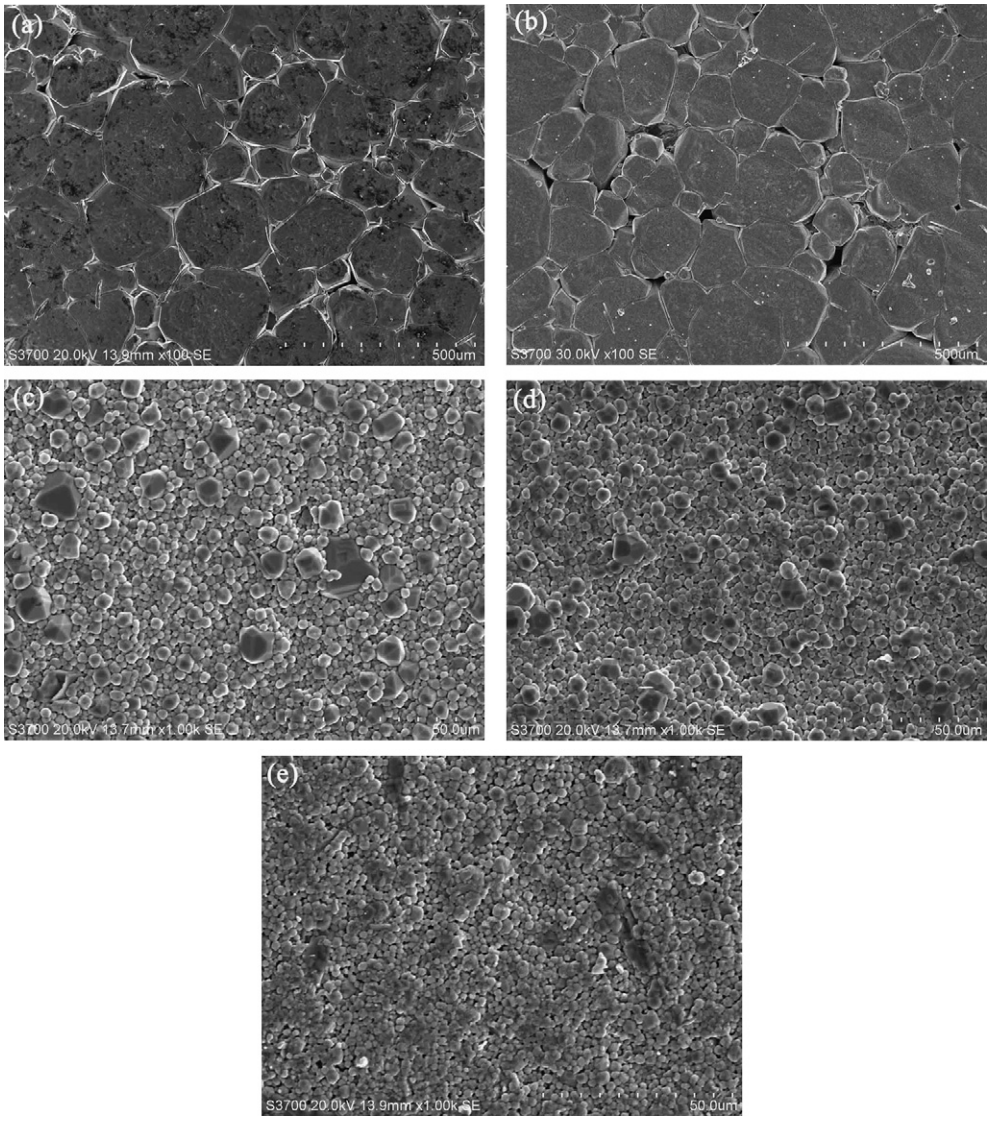

Fig. 3. Scanning electron micrographs of BZT ceramics with different Hf contents (a) 0 wt.%, (b) 0.5 wt.%, (c) 1.5 wt.%, (d) 2.0 wt.%, (e) 3.0 wt.%.

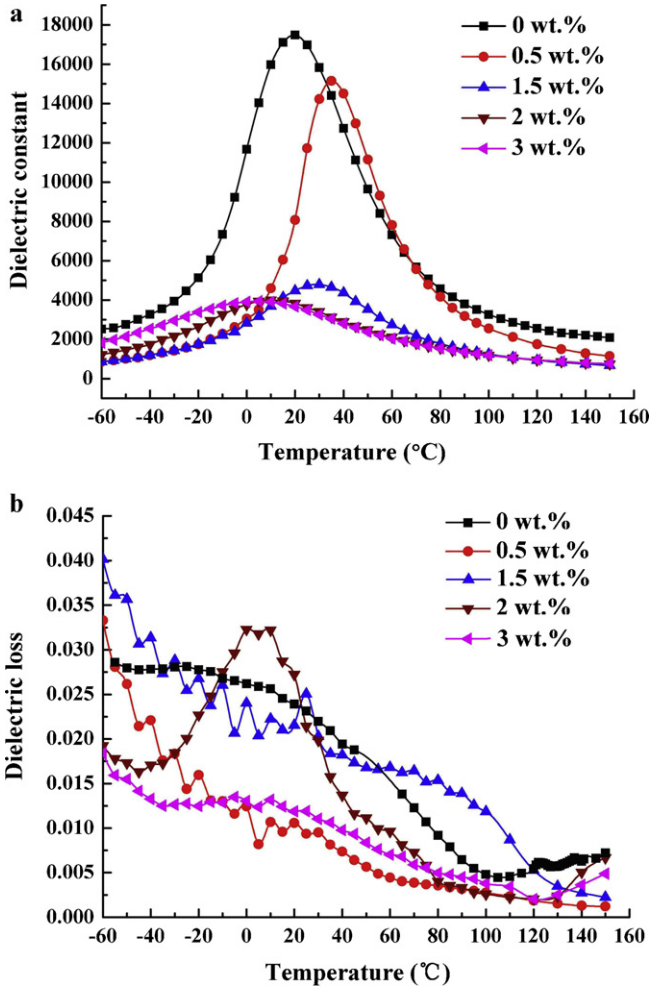

Fig. 4. The temperature dependence of dielectric properties of Hf-doped BZT ceramics measured at 1 kHz: (a) dielectric constant-*T*, (b) dielectric loss-*T*.

3.3. Dielectric properties

The temperature dependences of dielectric properties of Hf-doped BZT ceramics measured at 1 kHz are given in Fig. 4. It is found that the phase transition of the pure and Hf-doped BZT ceramics are quite diffuse, and the Curie temperature (T_C), corresponding to the maximum dielectric constant, of BZT ceramics with Hf dopant of 0 wt.%, 0.5 wt.%, 1.5 wt.%, 2.0 wt.% and 3.0 wt.%, is 20 °C, 40 °C, 35 °C, 15 °C, 10 °C, respectively. When Hf content is above 0.5 wt.%, the Curie temperature of BZT ceramics decreases with the increasing of Hf content. The change in the Curie temperature may be due to grain size. As the grain size decreases, the Curie temperature of Hf-doped BZT ceramics decreases. It is reported that the Curie temperature of BZT ceramics falls with the decreasing of the grain size [35,36]. According to SEM micrographs, the grain size of Hf-doped BZT ceramics decreases with the increasing of hafnium content. The grain size of BZT ceramics with 0.5 wt.% Hf is larger than that of the pure BZT ceramics, so the Curie temperature of BZT ceramics with 0.5 wt.% Hf is higher than that of the pure BZT ceramics. The maximum dielectric constant (ε_m) of Hf-doped BZT ceramics decreases with the increasing of Hf content. The reason for the decrease of the maximum dielectric constant is that the grain size decreases with the increasing of Hf content. As shown in Fig. 4(b), when the temperature is −30 to 60 °C, the dielectric loss of BZT ceramics with 0.5 wt.%, 1.5 wt.% and 3.0 wt.% Hf is lower than that of the pure BZT ceramics. The result indicates that the addition of Hf can decrease the dielectric loss of BZT ceramics. It is because that the chemical stability of Hf^{4+} is superior to that of Ti^{4+}. However, when the temperature is −10 to 30 °C, the dielectric loss of BZT ceramics with 2 wt.% Hf is higher than that of the pure BZT ceramics. It is due to the presence of dielectric loss peak.

Diffuse phase transition is generally characterized by broadening of the dielectric constant maximum at the phase transition temperature, a large separation between the maxima of dielectric constant and that of dielectric loss and a deviation from the Curie–Weiss law in the vicinity of T_C [36]. It is well known that the dielectric constant of a normal ferroelectric above the Curie temperature follows the Curie–Weiss law described by

$$\frac{1}{\varepsilon} = \frac{T - T_0}{C} \tag{2}$$

where T_0 is the Curie–Weiss temperature and C is the Curie–Weiss constant.

The parameter ΔT_m, which is often used to show the degree of the deviation from the Curie–Weiss law, is defined as follows:

$$\Delta T_m = T_{CW} - T_m \tag{3}$$

where T_{CW} denotes the temperature from which the permittivity starts to deviate from the Curie–Weiss law and T_m represents the temperature of dielectric constant maximum.

Fig. 5 shows the inverse of dielectric constant as a function of temperature at 1 kHz. The solid lines are plotted for the BZT ceramics with different Hf contents using Eq. (2) and some

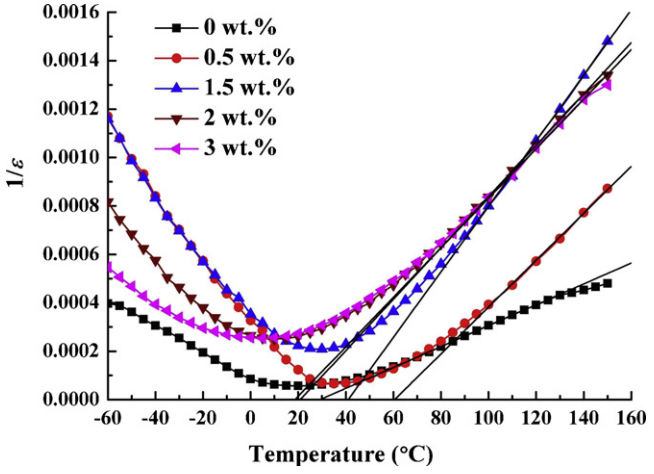

Fig. 5. Temperature dependence of the inverse dielectric constant for Hf-doped BZT ceramics at 1 kHz.

Table 1
The Curie–Weiss temperature (T_0), the Curie–Weiss constant (C), $T_{0.9\varepsilon_m}$, ΔT, T_{CW}, ΔT_m for Hf-doped BZT ceramics at 1 kHz.

Hf (wt.%)	0	0.5	1.5	2	3
T_0 (°C)	29.1	60.5	41	20.8	18.6
T_m (T_C) (°C)	20	35	30	10	5
C ($\times 10^5$ K)	2.320	1.033	0.739	0.944	0.978
ΔT (°C)	11	7	10	15	18
T_{CW} (°C)	60	105	100	90	95
ΔT_m (°C)	40	70	70	80	90
$T_{0.9\varepsilon_m}$ (°C)	31	42	40	25	23

parameters, such as T_0, C and T_{CW}, can be obtained from the fittings (listed in Table 1). It can be found that the dielectric behavior does not completely follow the Curie–Weiss law at temperature above the Curie temperature (T_C). A deviation from the Curie–Weiss law starting at T_{CW} can be seen and T_{CW} is different for various samples. ΔT_m of BZT ceramics with Hf dopant of 0 wt.%, 0.5 wt.%, 1.5 at.%, 2 wt.% and 3 wt.% is 40 °C, 70 °C, 70 °C, 80 °C and 90 °C, respectively. It indicates that hafnium can enhance the diffuseness of the phase transition of BZT ceramics.

The diffuseness of the phase transition can also be described empirically by a parameter ΔT, which is defined by the following equation:

$$\Delta T = T_{0.9\varepsilon_m}(1\,\text{kHz}) - T_{\varepsilon_m}(1\,\text{kHz}) \quad (4)$$

where ε_m is the maximum value of the dielectric constant and $T_{0.9\varepsilon_m}$ is the temperature corresponding to 90% of the dielectric constant maximum in the high-temperature side at 1 kHz. When $T > T_m$, $T_{0.9\varepsilon_m}$ can be obtained by fitting the ε–T curve utilizing the Lorentz-type function. ΔT of BZT ceramics with 0 wt.%, 0.5 wt.%, 1.5 wt.%, 2 wt.% and 3 wt.% Hf is 11 °C, 7 °C, 10 °C, 15 °C and 18 °C, respectively. This result further proves that hafnium can enhance the diffuseness of the phase transition of BZT ceramics when hafnium content is above critical concentration (1.5 wt.%).

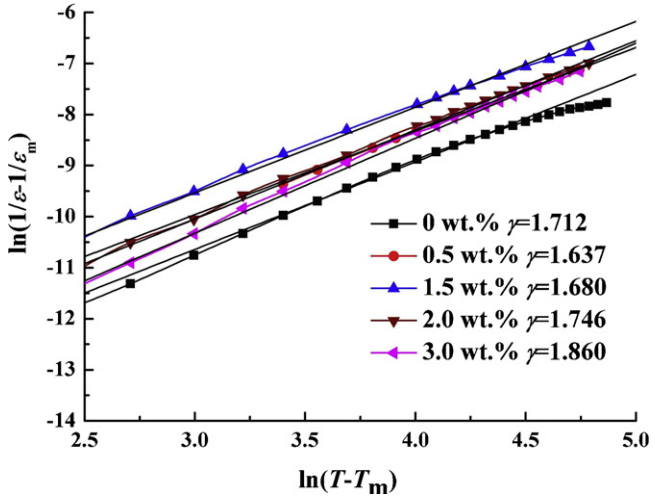

Fig. 6. Plot of $\ln(1/\varepsilon - 1/\varepsilon_m)$ as a function of $\ln(T - T_m)$ of the BZT ceramics with different Hf contents.

Table 2
The temperature (T_m) of dielectric constant maximum, the inverse maximum dielectric constant ($1/\varepsilon_m$) and the diffuseness constant (γ) for Hf-doped BZT ceramics.

Hf (wt.%)	0	0.5	1.5	2	3
T_m (°C)	20	35	30	10	5
$1/\varepsilon_m$ ($\times 10^{-4}$)	0.572	0.660	2.089	2.502	2.540
γ	1.712	1.637	1.680	1.746	1.860

A modified Curie–Weiss law was proposed to describe the diffuseness of the ferroelectric phase transition as [37]:

$$\frac{1}{\varepsilon} - \frac{1}{\varepsilon_m} = \frac{(T - T_m)^\gamma}{C'} \quad (5)$$

The plots of $\ln(1/\varepsilon - 1/\varepsilon_m)$ as a function of $\ln(T - T_m)$ for Hf-doped BZT ceramics are shown in Fig. 6. A linear relationship is observed for pure and Hf-doped BZT ceramics. The slope of the fitting curves using Eq. (5) is used to determine the γ value (listed in Table 2). It is found that as the hafnium content increases from 0 to 0.5 wt.%, 1.5 wt.%, 2 wt.% and 3 wt.%, the diffuseness constant γ decreases initially from 1.712 to 1.637, and then increases to 1.680, 1.746 and 1.860. It is evident that the diffuseness of the phase transition of Hf-doped BZT ceramics enhances when hafnium content is above 1.5 wt.%.

Fig. 7 shows dielectric constant and dielectric loss as a function of temperature at different frequencies for Hf-doped BZT ceramics. The dielectric constant peaks of pure and Hf-doped BZT ceramics decrease with the increase of frequency. There is no obvious frequency dispersion around the dielectric constant peaks for pure and Hf-doped BZT ceramics. It is indicated that Hf-doped BZT ceramics are not relaxor ferroelectrics but ferroelectrics with diffuse phase transition. Tang et al. [37] reported that the peak temperature (T_m) of dielectric constant would not shift with frequency when the dopant of Zr is lower than 25%. However, the content of Zr is more than 30%, T_m shifts with frequency following Vogel–Fulcher relation. The results of Fig. 6 are basically in agreement with the above reports. According to Fig. 7(a)–(e), the results can be described as follows: (1) The dielectric loss of pure and Hf-doped BZT ceramics decrease with the increase of temperature except that there is the peak of dielectric loss for BZT ceramics with 2.0 wt.% Hf at 1 kHz. It is because that the temperature is higher, the ferroelectric domain switch more easily under an alternating electric field. (2) When the temperature is below 0 °C, the dielectric loss decreases with the decrease of the frequency. Nevertheless, when the temperature is between 10 °C and 80 °C, the dielectric loss decreases with the increase of the frequency.

The frequency dependences of the dielectric constant and dielectric loss for Hf-doped BZT ceramics measured at room temperature are shown in Fig. 8. Firstly, it is found that the dielectric constant of BZT ceramics with different Hf

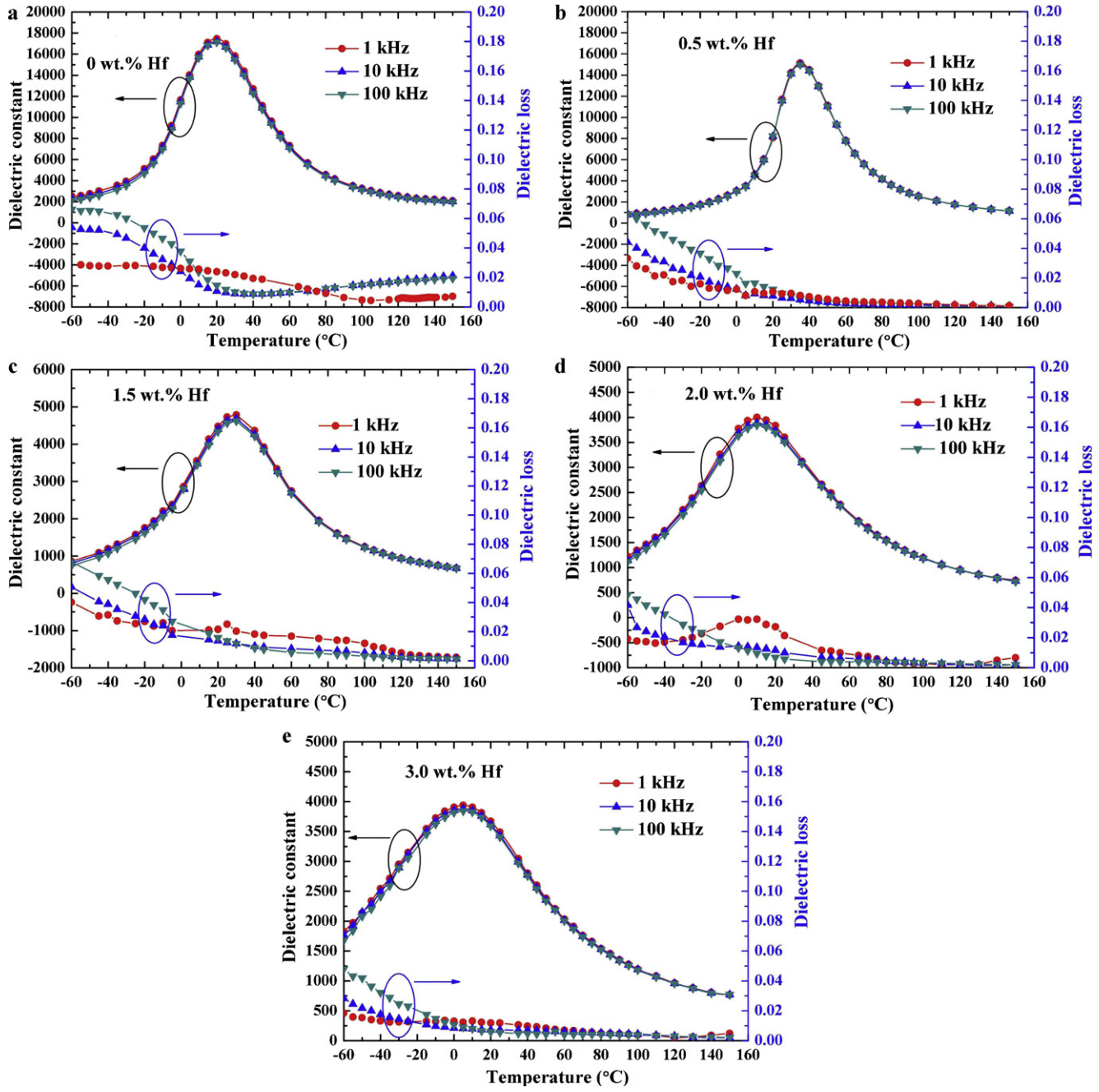

Fig. 7. Temperature dependence of dielectric constant and dielectric loss of Hf-doped BZT ceramics at different frequency: (a) 0 wt.% Hf, (b) 0.5 wt.% Hf, (c) 1.5 wt.% Hf, (d) 2.0 wt.% Hf, and (e) 3.0 wt.% Hf.

contents decreases with the increase of frequency. It is due to the different polarization mechanisms at different frequencies. At low frequency, electron displacement polarization, ion displacement polarization and turning-direction polarization contribute to dielectric constant. At high frequency, dielectric constant just results from the electron displacement polarization. Secondly, it is also found that the dielectric constant of Hf-doped BZT ceramics at different frequencies and room temperature decreases with the increase of Hf content. It is attributed to the effect of grain size on the dielectric constant. The dielectric constant of the grain is larger than that of the grain boundary. The grain size of the BZT ceramics with 0.5 wt.% Hf is the maximum, and the ratio of the grain boundary in samples is the minimum, hence the dielectric constant is the maximum. Thirdly, the dielectric loss of Hf-doped BZT ceramics decreases with the increase of frequency when the frequency is below 100 kHz. However, the dielectric loss gradually increases as frequency increases when the frequency is above 100 kHz. Furthermore, the dielectric loss of Hf-doped BZT ceramics decreases with the increment of Hf content at the higher frequency.

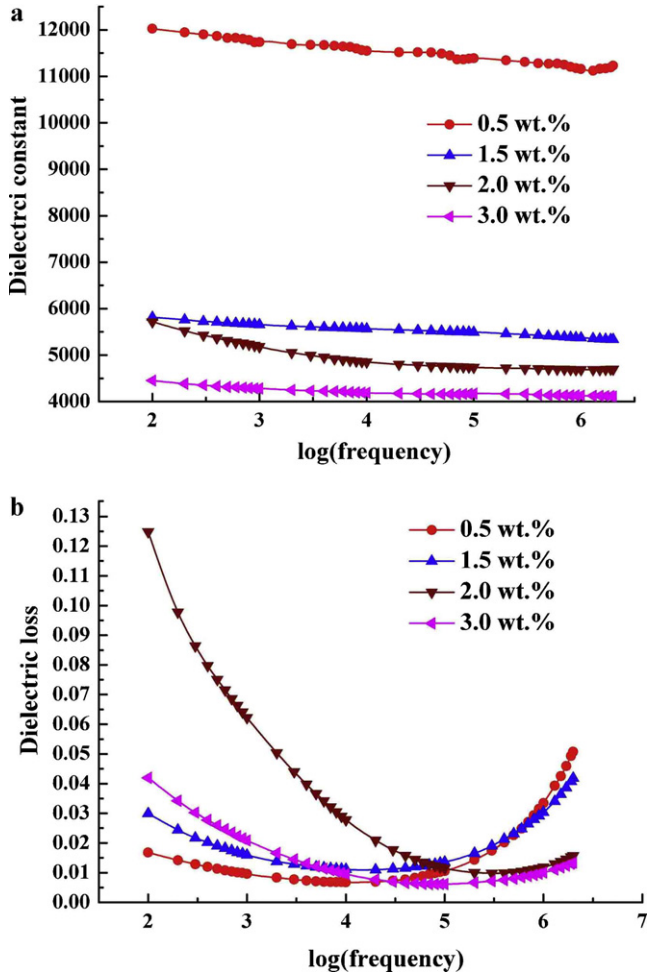

Fig. 8. Frequency dependence of dielectric constant and dielectric loss for Hf-doped BZT ceramics at room temperature.

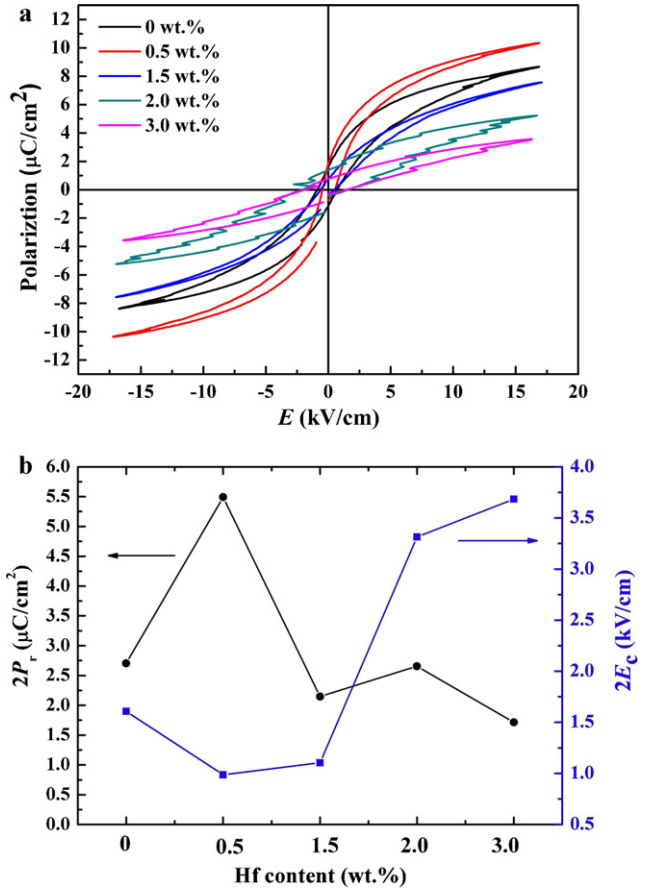

Fig. 9. Hysteresis loops of BZT ceramics with different Hf contents at 500 Hz.

3.4. Ferroelectric properties

Fig. 9 shows hysteresis loops of BZT ceramics with different Hf contents measured at room temperature and 500 Hz. The saturation *P–E* hysteresis loops confirm the ferroelectric nature of pure and Hf-doped BZT ceramics. The remnant polarization (P_r) begins to increase to the maximum (Hf content = 0.5 wt.%) and then decreases with the increasing of Hf content. It is due to grain size effect. The grain size of BZT ceramics with 0.5 wt.% Hf is the maximum. When Hf content is above 0.5 wt.%, the grain size of the sample decreases with the increasing of Hf content. The smaller grain size in Hf-doped BZT ceramics inhibits the formation of large ferroelectric domains, which reduces the effective contribution to total polarization [38]. Moreover, the Curie temperature for BZT ceramics with 2.0 wt.% and 3.0 wt.% are 10 °C and 5 °C, which is below the hysteresis measurement temperature. Beyond the Curie temperature, the amount of paraelectric phase in BZT ceramics with 2.0 wt.% and 3.0 wt.% Hf is very large and hence the remnant polarization is small. The coercive field (E_c) begins to decrease to the minimum (Hf content = 0.5 wt.%) and then increases with the increasing of Hf content. The result could be attributed to grain size. Energy barrier for switching ferroelectric domain must be broken through and it increases as grain size decreases. So the reversal polarization process of a ferroelectric domain is more difficult inside a small grain than in a large grain [39]. As mentioned above, the grain size of Hf-doped BZT ceramics begins to increase and then decreases with the increasing of hafnium content.

The polarization hysteresis loops of Hf-doped BZT ceramics measured at various temperatures are shown in Fig. 10. The remnant polarization (P_r), saturation polarization (P_s) and the coercive fields (E_c) decrease simultaneously with the rise of temperature. It is due to phase transition from ferroelectric to paraelectric. The ratio of paraelectric phase of Hf-doped BZT ceramics at higher temperature is more than that at lower temperature so that the remnant polarization decreases. The domain and domain wall can switch more easily at higher temperature, hence the coercive field decreases. However, when temperature is above T_m (T_m is 35 °C, 30 °C, 10 °C and 5 °C for 0.5 wt.%, 1.5 wt.%, 2.0 wt.% and 3.0 wt.% Hf, respectively), the remnant polarization is not zero and a nonlinear *P–E* behavior is present, implying that micropolar clusters exist above T_m which is a typical ferroelectric–relaxor characteristic [40]. The result further proves that there is diffuse phase transition and relaxor-like behavior in Hf-doped BZT ceramics.

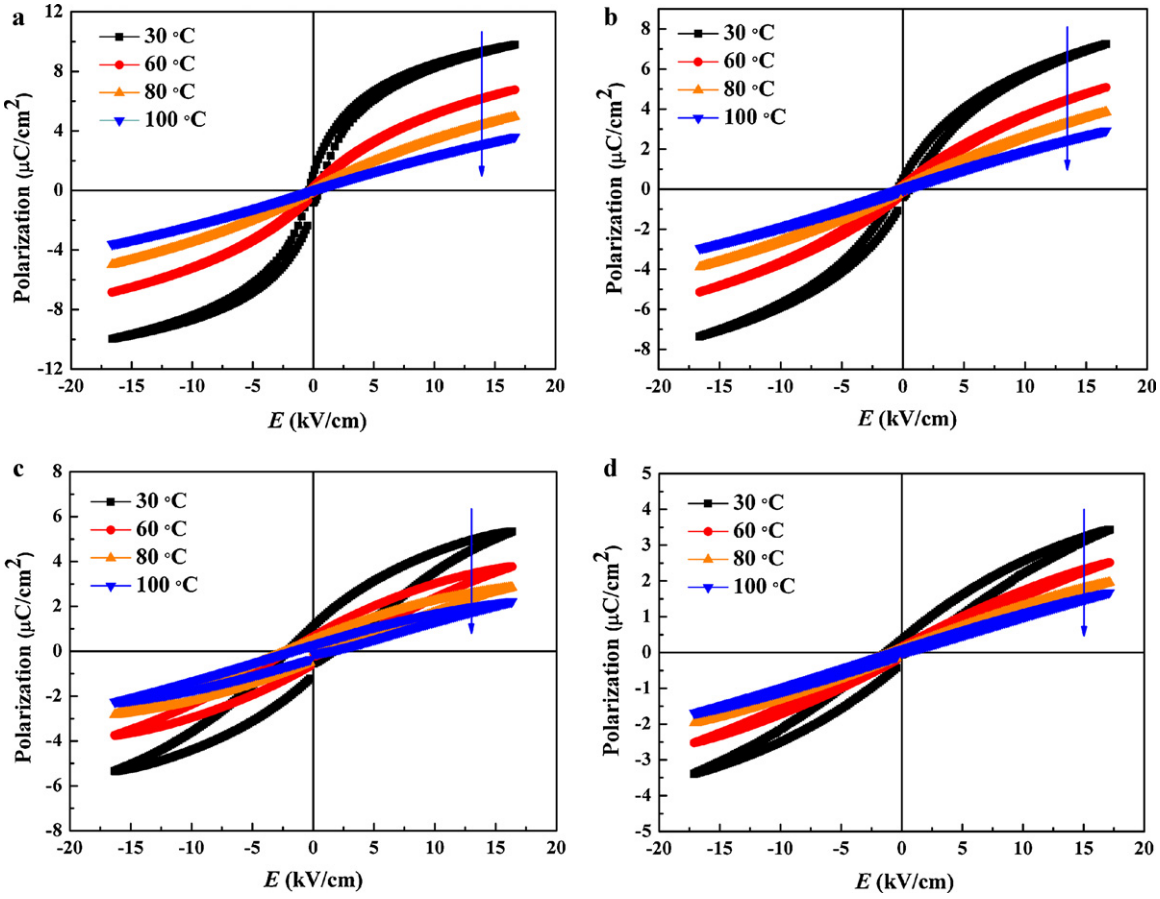

Fig. 10. Hysteresis loops of BZT ceramics with different Hf contents at various temperatures: (a) 0.5 wt.% Hf, (b) 1.5 wt.% Hf, (c) 2.0 wt.% Hf, and (d) 3.0 wt.% Hf.

4. Conclusions

In summary, crystal structure, surface morphology, dielectric and ferroelectric properties of Hf-doped $Ba[Zr_{0.2}Ti_{0.8}]O_3$ ceramics were investigated. XRD patterns indicate that the Hf-doped BZT ceramics have a single cubic phase. The lattice parameters increase with the increasing of Hf content. Addition of hafnium can restrain grain growth in the BZT ceramics and the grain size decrease sharply when Hf content is above 0.5 wt.%. Hf-doped BZT ceramics are not relaxor ferroelectrics but ferroelectrics with diffuse phase transition. Addition of hafnium can decrease the dielectric loss of BZT ceramics. As Hf content increases, the remnant polarization begins to increase to the maximum (Hf content = 0.5 wt.%) and then decreases, while the coercive field begins to decrease to the minimum (Hf content = 0.5 wt.%) and then increases. The remnant polarization, saturation polarization and coercive fields decrease simultaneously with the rise of measurement temperature.

Acknowledgments

This work was supported financially by the National Natural Science Foundation of China (Grant No. 51102288), Natural Science Foundation of Chongqing, China (Grant Nos. CSTC2010BB4286 and CSTC2011BA4027), Open Research Fund of State Key Laboratory of Electronic Thin Films and Integrated Devices (UESTC) (KFJJ201104) and Research Foundation of Chongqing University of Science and Technology (Grant No. CK2010Z05).

References

[1] W. Cai, C.L. Fu, Z.B. Lin, X.L. Deng, Vanadium doping effects on microstructure and dielectric properties of barium titanate ceramics, Ceramics International 37 (2011) 3643–3650.

[2] K. Niesz, T. Ould-Ely, H. Tsukamoto, D.E. Morse, Engineering grain size and electrical properties of donor-doped barium titanate ceramics, Ceramics International 37 (2011) 303–311.

[3] J.Z. Xin, C.W. Leung, H.L.W. Chan, Composition dependence of structural and optical properties of $Ba(Zr_x,Ti_{1-x})O_3$ thin films grown on MgO substrates by pulsed laser deposition, Thin Solid Films 519 (2011) 6313–6318.

[4] S.J. Kuang, X.G. Tang, L.Y. Li, Y.P. Jiang, Q.X. Liu, Influence of Zr dopant on the dielectric properties and Curie temperatures of $Ba(Zr_x$-$Ti_{1-x})O_3$ ($0 \leq x \leq 0.12$) ceramics, Scripta Materialia 61 (2009) 68–71.

[5] I.K. Jeong, C.Y. Park, J.S. Ahn, S. Park, D.J. Kim, Ferroelectric–relaxor crossover in $Ba(Ti_{1-x}Zr_x)O_3$ studied using neutron total scattering measurements and reverse Monte Carlo modeling, Physical Review B 81 (2010) 214119.

[6] T.M. Doan, L. Lu, M.O. Lai, Thickness dependence of structure, tunable and pyroelectric properties of laser-ablated $Ba(Zr_{0.25}Ti_{0.75})O_3$ thin films, Journal of Physics D: Applied Physics 43 (2010) 035402.

[7] X.Y. Chen, W. Cai, C.L. Fu, H.Q. Chen, Q. Zhang, Synthesis and morphology of $Ba(Zr_{0.20}Ti_{0.80})O_3$ powders obtained by sol–gel method, Journal of Sol–Gel Science and Technology 57 (2011) 149–156.
[8] N. Binhayeeniyi, P. Sukvisut, C. Thanachayanont, S. Muensit, Physical and electromechanical properties of barium zirconium titanate synthesized at low-sintering temperature, Materials Letters 64 (2010) 305–308.
[9] D. Richinschi, C.E. Ciomaga, L. Mitoseriu, V. Buscaglia, M. Okuyama, Ferroelectric–relaxor crossover characteristics in $Ba(Zr_xTi_{1-x})O_3$ ceramics investigated by AFM-piezoresponse study, Journal of the European Ceramic Society 30 (2010) 237–241.
[10] K.H. Chen, T.C. Chang, G.C. Chang, Y.E. Hsu, Y.C. Chen, H.Q. Xu, Low temperature improvement method on characteristics of $Ba(Zr_{0.1}Ti_{0.9})O_3$ thin films deposited on indium tin oxide/glass substrates, Applied Physics A 99 (2010) 291–295.
[11] L.N. Gao, J.W. Zhai, X. Yao, Influence of MgO and ZrO_2 buffer layers on dielectric properties of $Ba(Zr_{0.20}Ti_{0.80})O_3$ thin films prepared by sol–gel processing, Applied Surface Science 257 (2011) 3836–3839.
[12] X. Diez-Betriu, J.E. Garcia, C. Ostos, A.U. Boya, D.A. Ochoa, L. Mestres, R. Perez, Phase transition characteristics and dielectric properties of rare-earth (La, Pr, Nd, Gd) doped $Ba(Zr_{0.09}Ti_{0.91})O_3$ ceramics, Materials Chemistry and Physics 125 (2011) 493–499.
[13] S.B. Reddy, K.P. Rao, M.S.R. Rao, Influence of A-site Gd doping on the microstructure and dielectric properties of $Ba(Zr_{0.1}Ti_{0.9})O_3$ ceramics, Journal of Alloys and Compounds 509 (2011) 1266–1270.
[14] W. Cai, J.C. Gao, C.L. Fu, L.W. Tang, Dielectric properties, microstructure and diffuse transition of Ni-doped $Ba(Zr_{0.2}Ti_{0.8})O_3$ ceramics, Journal of Alloys and Compounds 487 (2009) 668–674.
[15] Y.L. Wang, L.T. Li, J.Q. Qi, Z.L. Gui, Ferroelectric characteristics of ytterbium-doped barium zirconium titanate ceramics, Ceramics International 28 (2002) 657–661.
[16] T. Badapanda, S.K. Rout, L.S. Cavalcante, J.C. Sczancoski, S. Panigrahi, T.P. Sinha, E. Longo, Structural and dielectric relaxor properties of yttrium-doped $Ba(Zr_{0.25}Ti_{0.75})O_3$ ceramics, Materials Chemistry and Physics 121 (2010) 147–153.
[17] T.A. Jain, K.Z. Fung, S. Hsiao, J. Chan, Effects of $BaO–SiO_2$ glass particle size on the microstructures and dielectric properties of Mn-doped Ba(Ti, Zr)O_3 ceramics, Journal of the European Ceramic Society 30 (2010) 1469–1476.
[18] P. Jarupoom, K. Pengpat, G. Rujijanagul, Enhanced piezoelectric properties and lowered sintering temperature of $Ba(Zr_{0.07}Ti_{0.93})O_3$ by B_2O_3 addition, Current Applied Physics 10 (2010) 557–560.
[19] F. Moura, A.Z. Simões, C.A. Paskocimas, M.A. Zaghete, J.A. Varela, E. Longo, Temperature dependence on the electrical properties of $Ba(Ti_{0.90}Zr_{0.10})O_3$:2 V ceramics, Materials Chemistry and Physics 123 (2010) 772–775.
[20] S. Mahajan, O.P. Thakur, D.K. Bhattacharya, K. Sreenivas, Ferroelectric relaxor behaviour and impedance spectroscopy of Bi_2O_3-doped barium zirconium titanate ceramics, Journal of Physics D: Applied Physics 42 (2009) 065413.
[21] P. Zheng, J.L. Zhang, S.F. Shao, Y.Q. Tan, C.L. Wang, Piezoelectric properties and stabilities of CuO-modified Ba(Ti,Zr)O_3 ceramics, Applied Physics Letters 94 (2009) 032902.
[22] L.N. Gao, J.W. Zhai, Y.W. Zhang, X. Yao, Influence of rare-earth addition on dielectric properties and relaxor behavior of barium zirconium titanate thin films, Journal of Applied Physics 107 (2010) 064105.
[23] R. Chourasia, O.P. Shrivastava, Crystal structure modeling, electrical and microstructural characterization of manganese doped barium zirconium titanate ceramics, Polyhedron 30 (2011) 738–745.
[24] X.J. Chou, J.W. Zhai, H.T. Jiang, X. Yao, Dielectric properties and relaxor behavior of rare-earth (La, Sm, Eu, Dy, Y) substituted barium zirconium titanate ceramics, Journal of Applied Physics 102 (2007) 084106.
[25] A. Aoujgal, W.A. Gharbi, A. Outzourhit, H. Ahamdane, A. Ammar, A. Tachafine, J.C. Carru, Relaxor behavior in $(Ba_{1-3x/2}Bi_x)(Zr_yTi_{1-y})O_3$ ceramics, Ceramics International 37 (2011) 2069–2074.
[26] W. Li, Z.J. Xu, R.Q. Chu, P. Fu, G.Z. Zang Piezoelectric, Dielectric properties of $(Ba_{1-x}Ca_x)(Ti_{0.95}Zr_{0.05})O_3$ lead-free ceramics, Journal of the American Ceramic Society 93 (2010) 2942–2944.
[27] S. Halder, P. Gerber, T. Schneller, R. Waser, Structural, dielectric and electromechanical study of Hf-substituted $BaTiO_3$ thin films fabricated by CSD, Applied Physics A 83 (2006) 285–288.
[28] J.F. Ihledeld, W.J. Borland, J.P. Maria, Dielectric and microstructural properties of barium titanate hafnate thin films, Thin Solid Films 516 (2008) 3162–3166.
[29] S. Anwar, P.R. Sagdeo, N.P. Lalla, Ferroelectric relaxor behavior in hafnium doped barium-titanate ceramic, Solid State Communications 138 (2006) 331–336.
[30] S. Anwar, P.R. Sagdeo, N.P. Lalla, Locating the normal to relaxor phase boundary in $Ba(Ti_{1-x}Hf_x)O_3$ ceramics, Materials Research Bulletin 43 (2008) 1761–1769.
[31] L.S. Cavalcante, J.C. Sczancoski, F.S. De Vicente, M.T. Frabbro, M. Siu Li, J.A. Varela, E. Longo, Microstructure, dielectric properties and optical band gap control on the photoluminescence behavior of $Ba[Zr_{0.25}Ti_{0.75}]O_3$ thin films, Journal of Sol–Gel Science and Technology 49 (2009) 35–46.
[32] T. Badapanda, V. Senthil, S.K. Rout, L.S. Cavalcante, A.Z. Simões, T.P. Sinha, S. Panigrahi, M.M. de Jesus, E. Longo, J.A. Varela, Rietveld refinement, microstructure, conductivity and impedance properties of $Ba[Zr_{0.25}Ti_{0.75}]O_3$ ceramic, Current Applied Physic 11 (2011) 1282–1293.
[33] S. Halder, T. Schneller, R. Waser, S.B. Majumder, Electrical and optical properties of chemical solution deposited barium hafnate titanate thin films, Thin Solid Films 516 (2008) 4970–4976.
[34] H.Y. Tian, Y. Wang, J. Miao, H.L.W. Chan, C.L. Choy, Preparation and characterization of hafnium doped barium titanate ceramics, Journal of Alloys and Compounds 431 (2007) 197–202.
[35] S.B. Reddy, M.S.R. Rao, K.P. Rao, Observation of high permittivity in Ho substituted $BaZr_{0.1}Ti_{0.9}O_3$ ceramics, Applied Physics Letters 91 (2007) 022917.
[36] X.G. Tang, J. Wang, X.X. Wang, H.L.W. Chan, Effects of grain size on the dielectric properties and tunabilities of sol–gel derived $Ba(Zr_{0.2}Ti_{0.8})O_3$ ceramics, Solid State Communications 131 (2004) 163–168.
[37] X.G. Tang, K.H. Chew, H.L.W. Chan, Diffuse phase transition and dielectric tunability of $Ba(Zr_yTi_{1-y})O_3$ relaxor ferroelectric ceramics, Acta Materialia 52 (2004) 5177–5183.
[38] J.W. Zhai, X. Yao, J. Shen, L.Y. Zhang, H. Chen, Structural and dielectric properties of $Ba(Zr_xTi_{1-x})O_3$ thin films grown by a sol–gel process, Journal of Physics D: Applied Physics 7 (2004) 748–752.
[39] C.C. Leu, C.Y. Chen, C.H. Chien, M.N. Chang, F.Y. Hsu, C.T. Hu, Domain structure study of $SrBi_2Ta_2O_9$ ferroelectric thin films by scanning capacitance microscopy, Applied Physics Letters 82 (2003) 3493.
[40] Z. Yu, C. Ang, R.Y. Guo, A.S. Bhalla, Ferroelectric–relaxor behavior of $Ba(Ti_{0.7}Zr_{0.3})O_3$ ceramics, Journal of Applied Physics 92 (2002) 2655.